

Copyright © 2015 by Academic Publishing House *Researcher*

Published in the Russian Federation  
European Journal of Molecular Biotechnology  
Has been issued since 2013.  
ISSN: 2310-6255  
E-ISSN 2409-1332  
Vol. 8, Is. 2, pp. 63-79, 2015

DOI: 10.13187/ejmb.2015.8.63  
[www.ejournal8.com](http://www.ejournal8.com)



UDC 553.9: 470.22

### Studying the Mechanism of Phototransformation of Light Signal by Various Mammal and Bacterial Photoreceptor Pigments – Rhodopsin, Iodopsin and Bacteriorhodopsin

<sup>1</sup> Ignat Ignatov  
<sup>2</sup> Oleg Mosin

<sup>1</sup> The Scientific Research Center of Medical Biophysics (SRC MB), Bulgaria  
Professor, D.Sc., director of SRC MB  
1111, Sofia, N. Kopernik street, 32  
E-mail: mbioph@dir.bg

<sup>2</sup> Moscow State University of Applied Biotechnology, Russian Federation  
Senior research Fellow of Biotechnology Department, Ph. D. (Chemistry)  
103316, Moscow, Talalihin ulitsa, 33  
E-mail: mosin-oleg@yandex.ru

#### Abstract

This review article outlines the structure and function of mammal and bacterial photoreceptor pigments (rhodopsin, iodopsin, bacteriorhodopsin) and their aspects of biotechnological usage. On an example of bacteriorhodopsin is described the method of its isolation from purple membranes of photo-organotrophic halobacterium *Halobacterium halobium* ET 1001 by cellular autolysis by distilled water, processing of bacterial biomass by ultrasound at 22 KHz, alcohol extraction of low and high-weight molecular impurities, cellular RNA, carotenoids and lipids, the solubilization with 0,5 % (w/v) SDS-Na and subsequent fractionation by methanol and gel filtration chromatography on Sephadex G-200 Column balanced with 0,09 M Tris-buffer (pH = 8,35) with 0,1 % (w/v) SDS-Na and 2,5 mM EDTA. Within the framework of the research the mechanism of color perception by the visual retina analyzer having the ability to analyze certain ranges of the optical spectrum as colors, was studied along with an analysis of the additive mixing of two or more colors. It was shown that at the mixing of electromagnetic waves with different wavelengths, the visual analyzer perceives them as the separate or average wave length corresponding to the mixing color.

**Keywords:** vision, rhodopsin, iodopsin, bacteriorhodopsin, additive colour mixing.

#### Introduction

Vision (the visual perception) is a process of psycho-physiological processing of the images of surrounding objects, carried out by the visual system, which allows get an idea of the size, shape and color of surrounding objects, their relative position and distance between them. By means of this mechanism the mammals can receive 90 % of all incoming visual information to the brain.

The function of the visual system is carried out through various interrelated complex structures designated as retina visual analyzer, consisting of a peripheral part (retina, optic nerve, optical tract) and the central department of combining stem and subcortical centers of the midbrain, as well as the visual cortex of the cerebral hemispheres. It is known that the human eye can perceive only light waves of a certain length – from  $\lambda = 380$  to  $\lambda = 770$  nm.

The light rays from treated subjects pass through the optical system of the eye (cornea, lens and vitreous body) and onto the retina, wherein the light-sensitive photoreceptor cells (rods and cones) are located. Light incidented on the photoreceptors, triggers a cascade of biochemical reactions of visual pigments (in particular, the most studied of them is the mammal retina pigment, rhodopsin responsible for the perception of electromagnetic radiation in the visible range), and in turn, – the occurrence of nerve impulses, which are transmitted through the following retinal neurons and further to the optic nerve. The optic nerve in turn carries the nerve impulses into the lateral geniculate body – subcortical center of vision, and thence to the cortical center, located in the occipital lobe of the brain, where the visual image is formed.

Over the last decade new data have been obtained, revealing the molecular basis of visual perception. The visual molecules of mammals (rhodopsin, iodopsin) and halobacteria (bacteriorhodopsin), involved in the light perception, were identified and the mechanism of their action recently was cleared up quite completely.

The structural research of rhodopsin and its affiliated chromophore proteins of eukaryotic and prokaryotic origin (iodopsin, bacteriorhodopsin) and the analysis of their functioning have been carried out in the Scientific Research Center of Medical Biophysics (Bulgaria) throughout the last 20 years. These studies have been aimed at finding new effective methods based on biotechnology for better treatment of ophthalmic diseases.

The purpose of the research was the studying of basic biochemical mechanisms associated with visual perception of light by the mammal phototransforming pigment rhodopsin and some nano- and biotechnological applications of visual phototransforming pigments as trans-membrane protein bacteriorhodopsin, extracted from purple membranes of photo-organotrophic halobacterium *Halobacterium halobium ET 1001*.

## Material and Methods

### Biological objects

As a producer of bacteriorhodopsin (BR) was used a carotenoid strain of extreme photo-organotrophic halobacterium *Halobacterium halobium ET 1001*, obtained from Moscow State University (Russia). The strain was modified by selection of individual colonies on solid (2 % (w/v) agarose) media with peptone and 4,3 M NaCl.

### Growth conditions

BR (yield 8–10 mg from 1 g of raw biomass) was obtained in synthetic (SM) medium (g/l): *D,L*-alanine – 0,43; *L*-arginine – 0,4; *D,L*-aspartic acid – 0,45; *L*-cysteine – 0,05; *L*-glutamic acid – 1,3; *L*-lysine – 0,06; *D,L*-histidine – 0,3; *D,L*-isoleucine – 0,44; *L*-leucine – 0,8; *L*-lysine – 0,85; *D,L*-methionine – 0,37; *D,L*-phenylalanine – 0,26; *L*-proline – 0,05; *D,L*-serine – 0,61; *D,L*-threonine – 0,5; *L*-tyrosine – 0,2; *D,L*-tryptophan – 0,5; *D,L*-valine – 1,0; AMP – 0,1; UMP – 0,1; NaCl – 250;  $\text{MgSO}_4 \cdot 7\text{H}_2\text{O}$  – 20; KCl – 2;  $\text{NH}_4\text{Cl}$  – 0,5;  $\text{KNO}_3$  – 0,1;  $\text{KH}_2\text{PO}_4$  – 0,05;  $\text{K}_2\text{HPO}_4$  – 0,05;  $\text{Na}^+$ -citrate – 0,5;  $\text{MnSO}_4 \cdot 2\text{H}_2\text{O}$  –  $3 \cdot 10^{-4}$ ;  $\text{CaCl}_2 \cdot 6\text{H}_2\text{O}$  – 0,065;  $\text{ZnSO}_4 \cdot 7\text{H}_2\text{O}$  –  $4 \cdot 10^{-5}$ ;  $\text{FeSO}_4 \cdot 7\text{H}_2\text{O}$  –  $5 \cdot 10^{-4}$ ;  $\text{CuSO}_4 \cdot 5\text{H}_2\text{O}$  –  $5 \cdot 10^{-5}$ ; glycerol – 1,0; biotin –  $1,0 \cdot 10^{-4}$ ; folic acid –  $1,5 \cdot 10^{-4}$ ; vitamin  $\text{B}_{12}$  –  $2 \cdot 10^{-5}$ . The growth medium was autoclaved for 30 min at 0,5 atm, the *pH* value was adjusted to 6,5–6,7 with 0,5 M KOH. Bacterial growth was performed in 500 ml Erlenmeyer flasks (volume of the reaction mixture 100 ml) for 4–5 days at +35 °C on Biorad shaker (“Biorad Labs”, Hungary) under intense aeration and monochromatic illumination (3 lamps  $\times$  1,5 lx). All further manipulations for BR isolation were carried out with the use of a photomask lamp equipped with an orange light filter.

### Isolation of purple membranes (PM)

Biomass (1 g) was washed with distilled water and pelleted by centrifugation on T-24 centrifuge (“Carl Zeiss”, Germany) (1500 g, 20 min). The precipitate was suspended in 100 ml of dist.  $\text{H}_2\text{O}$  and kept for 3 h at +4 °C. The reaction mixture was centrifuged (1500 g, 15 min), the

pellet was resuspended in 20 ml dist. H<sub>2</sub>O and disintegrated by infrasound sonication (22 kHz, 3 times × 5 min) in an ice bath (0 °C). The cell homogenate after washing with dist. H<sub>2</sub>O was resuspended in 10 ml of buffer containing 125 mM NaCl, 20 mM MgCl<sub>2</sub>, and 4 mM Tris-HCl (pH = 8,0), then 5 mg of RNA-ase (2–3 units of activity) was added. The mixture was incubated for 2 h at +37 °C. Then 10 ml of the same buffer was added and kept for 10–12 h at 4 °C. The aqueous fraction was separated by centrifugation (1500 g, 20 min), the PM precipitate was treated with 50 % (v/v) ethanol (5 times × 7 ml) at +4 °C followed by separation of the solvent. This procedure was repeated 6 times to give colorless washings. The protein content in the samples was determined spectrophotometrically on DU-6 spectrophotometer (“Beckman Coulter”, USA) by the ratio  $D_{280}/D_{568}$  ( $\epsilon_{280} = 1,1 \cdot 10^5$ ;  $\epsilon_{568} = 6,3 \cdot 10^4 \text{ M}^{-1} \cdot \text{cm}^{-1}$ ) [1]. PM regeneration is performed as described in [2]. Yield of PM fraction was 120 mg (80–85%).

### ***Isolation of BR***

The fraction of PM (in H<sub>2</sub>O) (1 mg/ml) was dissolved in 1 ml of 0,5 % (w/v) sodium dodecyl sulfate (SDS-Na), and incubated for 5–7 h at +37 °C followed by centrifugation (1200 g, 15 min). The precipitate was separated, then methanol was added to the supernatant in divided portions (3 times × 100 ml) at 0 °C. The reaction mixture was kept for 14–15 h in ice bath at +4 °C and then centrifuged (1200 g, 15 min). Fractionation procedure was performed three times, reducing the concentration of 0,5 % SDS-Na to 0,2 and 0,1 %. Crystal protein (output 8–10 mg) was washed with cold <sup>2</sup>H<sub>2</sub>O (2 times × 1 ml) and centrifuged (1200 g, 15 min).

### ***Purification of BR***

Protein sample (5 mg) was dissolved in 100 ml of buffer solution and placed on a column (150×10 mm), stationary phase – Sephadex G-200 (“Pharmacia”, USA) (specific volume packed beads – 30–40 units per 1 g dry. Sephadex) equilibrated with buffer containing 0,1 % (w/v) SDS-Na and 2,5 mM EDTA. Elution proceeded by 0,09 M Tris-HCl buffer containing 0,5 M NaCl, pH = 8,35 at a flow rate of 10 ml/cm<sup>2</sup>·h. The combined protein fraction was subjected to freeze-drying, in sealed glass ampoules (10×50 mm) and stored in frost camera at -10 °C.

### ***Quantitative analysis of the protein***

The process was performed in 12,5% (w/v) polyacrylamide gel (PAAG) containing 0,1 % (w/v) SDS-Na. The samples were prepared for electrophoresis by standard procedures (LKB protocol, Sweden). Electrophoretic gel stained with Coomassie blue R-250 was scanned on a CDS-200 laser densitometer (Beckman, USA) for quantitative analysis of the protein.

### ***Absorption spectrometry***

Absorption spectra of pigments were recorded on programmed DU-6 spectrophotometer (“Beckman Coulter”, USA) at  $\lambda = 280 \text{ nm}$  and  $\lambda = 750 \text{ nm}$ .

### ***IR-spectroscopy***

IR-spectra were registered on Bruker Vertex IR spectrometer (“Bruker”, Germany) (a spectral range: average IR – 370–7800 cm<sup>-1</sup>; visible – 2500–8000 cm<sup>-1</sup>; the permission – 0,5 cm<sup>-1</sup>; accuracy of wave number – 0,1 cm<sup>-1</sup> on 2000 cm<sup>-1</sup>) and Thermo Nicolet Avatar 360 Fourier-transform IR.

### ***Color analyzing***

Colors were analyzed by using chromatic color analyzer “Tsvetan” (“Photopribor”, Cherkassk, Ukraine). Operating relative absorbance, % from -80 to 70; measurement error, ±5 %; response time, from 0,4 sec to 63,0 sec; overall dimensions, 300 mm.

### ***Scanning electron microscopy***

The structural studies were carried out with using scanning electron microscopy (SEM) on JSM 35 CF (JEOL Ltd., Corea) device, equipped with X-ray microanalyzer “Tracor Northern TN”, SE detector, thermomolecular pump, and tungsten electron gun (Harpin type W filament, DC

heating): working pressure –  $10^{-4}$  Pa ( $10^{-6}$  Torr); magnification – 300000; resolution – 3,0 nm; accelerating voltage – 1–30 kV; sample size – 60–130 nm.

## Results and Discussion

### ***Practical aspects of molecular basis of vision***

The process of perception of light has a definite localization in photoreceptor light-sensitive cells of the retina. The retina in its structure is a multilayer layer of nervous tissue that is sensitive to light, which lines the inside of the back of the eyeball. Pigmented retina located at the membrane referred to as retinal pigmented epithelium (RPE), which absorbs light passing through the retina. This prevents the reverse reflection of the light through the retina and does not allow the vision to disperse.

Light enters through the eye and creates a complex of biochemical reactions in the photoreceptor cells of the retina. Photoreceptor cells are divided into two types that due to their characteristic form are designated as rods and cones [3]. Rods are receptors of light of low intensity; they arranged in a colored layer of the retina, in which is synthesized photochromic protein rhodopsin, responsible for color perception. Cones on the contrary contain a group of visual pigments (iodopsin), and adapted to distinguish different colors. Rods can perceive black and white images in the dim light, cones – to carry out color vision in bright light. Human retina contains approximately 3 million of cones and 100 million of rods. Their dimensions are very small – the length of about 50 nm, the diameter from 1 to 4  $\mu\text{m}$ .

Electrical signals generated by the rods and cones, are handled by other retina cells – bipolar and ganglion cells before they are transmitted to the brain via the optic nerve [4]. Additionally, there are two intermediate layers of neurons. Horizontal cells transmit messages back and forth between the photoreceptor cells, bipolar cells and each other. Amacrine cells of the retina are linked to bipolar cells, ganglion cells, as well as with each other. Both types of these intermediate neurons play a major role in the processing of visual information at the level of the retina before it is transmitted to the brain for final processing.

Cones are approximately 100 times less sensitive to light than rods, but much better perceive the rapid movement. The wand can be stimulated by a single photon. Cascade of molecular interactions enhances this “quantum” of information into a chemical signal, which is then perceived by the nervous system. The degree of enhancement signal varies depending on ambient light: rods are more sensitive under low than under bright light. As a result, they operate effectively in a wide range of ambient light. Sensory system of rods is packed up in clearly distinguishable cellular substructure that can be easily selected and investigated *in vitro* in isolated state. This property makes them as indispensable convenient objects for further structural-functional studies, as well as studies of photoreceptor pigments (rhodopsin, iodopsin) and the mechanism of their action. These mammal photoreceptor pigments are used as basic models for comparative studying the mechanism of light perception by the bacterial photoreceptor pigment bacteriorhodopsin (BR), isolated from purple membranes of halobacterium *Halobacterium halobium* ET 1001, since the mechanisms of perception of light by eukaryotes and halobacteria have some similar reactions.

### ***Rhodopsin and its structural and functional properties***

Rhodopsin [5] is one of the most important integral mammal photoreceptor proteins of rod retina cells, which absorbs a photon and creates a biochemical response constituting a first step in a chain of events that provide vision. Rhodopsin consists of two components – a colorless protein opsin and a chromophore component 11-*cis*-retinal residue, acted as the light acceptor (Fig. 1). The absorption of a light photon by 11-*cis*-retinal “turns on” the enzymatic activity of opsin and further photosensitive biochemical cascade of reactions that are responsible for vision [6].

Rhodopsin belongs to the group of the G-protein-coupled receptors (GPCR-receptors) of the retinylidene protein family responsible for transmembrane signaling mechanism based on the interaction with intracellular membrane G-proteins – universal intermediaries in the transmission of hormonal signals from the cell membrane receptors to effector proteins, causing the final cellular response. The establishment of the spatial structure of rhodopsin is so important because rhodopsin as the “originator” of the family of GPCR-receptors is a “model” for the structure and function of other receptors that it is extremely important from fundamental scientific and practical points of view [7].

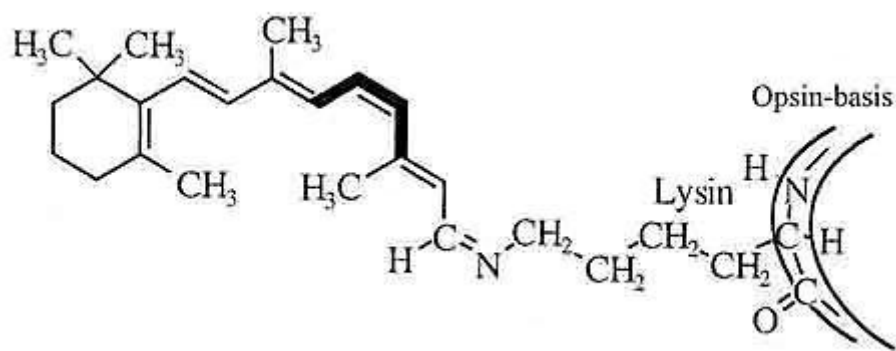


*Figure 1.* Configuration of photosensitive chromophore of rhodopsin in the basic (unexcited) phase (at the double bond is marked 11-*cis*-configuration)

The spatial structure of rhodopsin was defined by using X-ray diffraction and NMR spectroscopy, while the molecular structure of related to rhodopsin transmembrane chromoprotein bacteriorhodopsin (BR) [8] having a similar structure, performing the functions of ATP-dependent translocase in cell membranes of halophilic microorganisms pumped protons across the cytoplasmic membrane of the cell and is involved in the anaerobic photosynthetic phosphorylation (non-green synthesis), was determined as early as 1990. On the contrary, the complete structure of rhodopsin remained unknown until 2003 [9]. The opsin fragment of the rhodopsin molecule has 348 amino acid residues in a polypeptide chain that is formed by seven transmembrane  $\alpha$ -helix segments situated across the membrane and joined with short non-helix sections [10]. The N-terminus of  $\alpha$ -helix is located in the extracellular region, while the C-terminus – in the cytoplasmic region. The 11-*cis*-retinal residue is connected to one of the  $\alpha$ -helices, located near the middle of the membrane, so that its long axis is parallel to the membrane surface (Fig. 2). It was also determined the dislocation of 11-*cis*-retinal aldimine bond with  $\epsilon$ -amino group of Lys-296 residue being located in the seventh  $\alpha$ -helix. Thus, 11-*cis*-retinal is mounted in the center of a complex highly organized protein in the cellular membrane comprising rods. This rigid structure provides a photochemical “adjustment” of retinal residue, affecting its absorption spectrum. The free 11-*cis*-retinal in a dissolved form has an absorption maximum in the ultraviolet region – at a wavelength of 380 nm, while rhodopsin absorbs green light at 500 nm [11]. This shift in the wavelength of light is important from a functional point of view; it is aligned with the spectrum of light that enters into the retina.

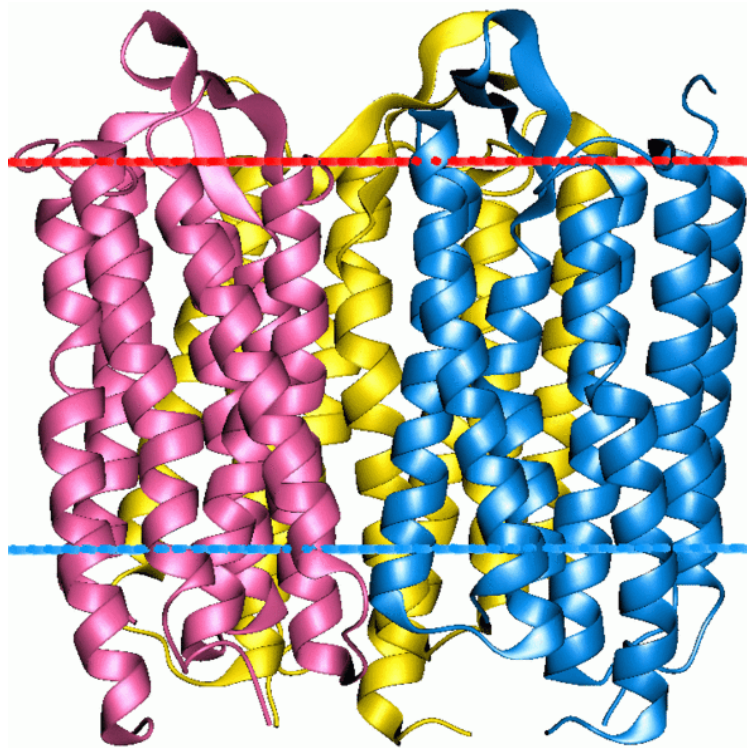


Figure 2. The structure of rhodopsin according to computer modeling data

The absorption spectrum of rhodopsin is defined by specific properties of the chromophore – 11-*cis*-retinal residue and opsin fragment. This range in vertebrates has two characteristic peaks – one in the ultraviolet ( $\lambda = 278$  nm) due to the opsin fragment, and the other – in the visible region ( $\lambda = 500$  nm) corresponds to absorption of the chromophore (Fig. 3). Further transformation of rhodopsin under the action of light to the final stable product consists of a series of very fast intermediate stages. Investigating the absorption spectra of intermediates of rhodopsin in retina extracts at low temperatures at which these products are stable, allows evaluate in the detail the photochemical changes of rhodopsin [12].

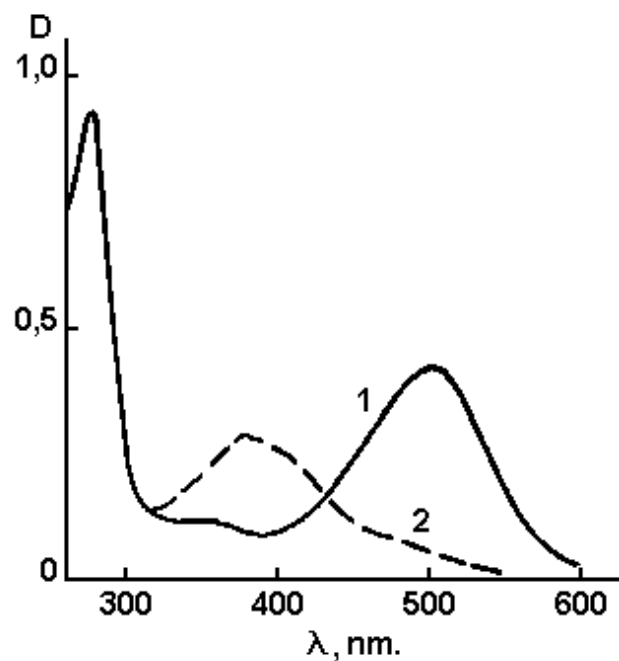
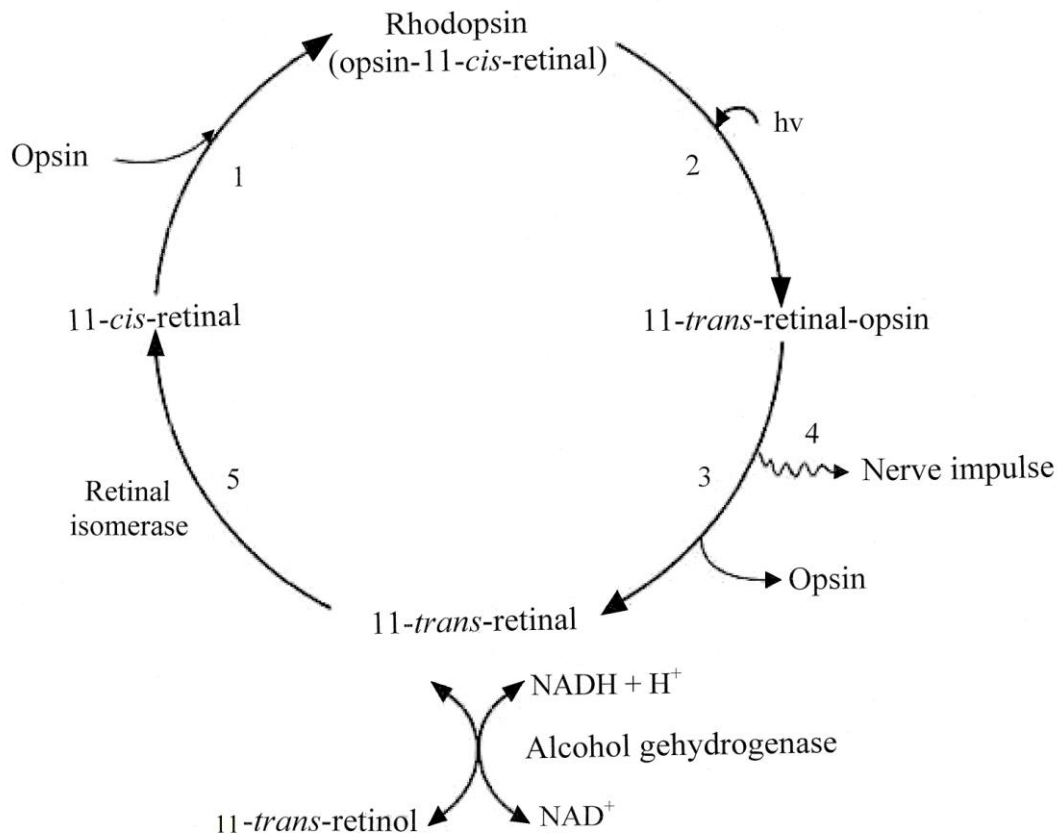


Figure 3. Absorption spectrum of rhodopsin from the frog *Rana temporaria* (in water extract):  
1 – rhodopsin (restored pigment); 2 – yellow indicator (discolored pigment)

Upon absorption of light photon it is occurred isomerization of 11-*cis*-retinal into 11-*trans*-retinal (quantum yield, 0,67), that induces a conformational change in the protein and activates photopsin and promotes its binding to G-protein transducin, which triggers a second messenger cascade [13]. Subsequent cycles of the photochemical reactions of rhodopsin lead to a local depolarization of the membrane and the stimulation of the nerve impulse propagates along the nerve fiber due to changes in ion transport in the photoreceptor (Fig. 4). Subsequently rhodopsin is restored (regenerated) with participation of retinal isomerase through the following steps, shown on Fig. 4: 11-*trans*-retinal → 11-*trans*-retinol → 11-*cis*-retinol → 11-*cis*-retinal, the latter is connected with opsin to form rhodopsin.



**Figure 4.** Photocycle scheme of rhodopsin: 1 – 11-*cis*-retinal in the dark links with protein opsin to form rhodopsin; 2 – under light illumination occurs photoisomerization of 11-*cis*-retinal into 11-*trans*-retinal; 3 – 11-*trans*-retinal-opsin complex splits into 11-*trans*-retinal and opsin; 4 – local depolarization of the membrane and the occurrence of a nerve impulse propagates along the nerve fiber; 5 – regeneration of the original pigment.

### ***Bacteriorhodopsin and its applications***

Bacteriorhodopsin (BR), named by analogy to the visual apparatus of mammalian chromoprotein rhodopsin, was isolated from the cell membrane of an extreme photo-organotrophic halobacterium *Halobacterium halobium* in 1971 by D. Osterhelt and W. Stohenius. This photo-transforming trans-membrane protein with the molecular weight ~26,5 kDa is a chromoprotein determining the purple-red colour of halophilic bacteria, contained as chromophore group an equimolar mixture of 13-*cis*- and 13-*trans*-retinol C<sub>20</sub>-carotenoid, bound by Schiff base (as in the visual animal pigments) with Lys-216 residue of the protein.

In its structure and location in the cell membrane BR refers to integral transmembrane proteins, penetrating the cell membrane, which is divided into three fractions: yellow, red and purple. Purple fraction comprising on 75% (w/w) of cell membrane consists from carotenoids, phospholipids (mostly phosphoglycerol diesters with a small amount of nonpolar lipids and isoprenoids) forms natural two-dimensional crystals which can be investigated using electron



microscopy diffraction methods as X-ray scattering [15]. These methods have established the existence in the BR molecule seven  $\alpha$ -helical protein segments, while in the middle are symmetrically located a retinal residue (Fig. 5).



*Figure 5.* The structure of BR from PM of halophilic bacterium *H. halobium* according to computer modeling data

Polypeptide chain of BR consists of 248 amino acid residues, 67% of which are hydrophobic, formed with the aromatic amino acids, and 33% – hydrophilic residues of aspartic and glutamic acids, arginine and lysine [16]. These residues play important structural and functional role in the spatial orientation of the  $\alpha$ -helical segments of the BR molecule, arranged in PM in an orderly manner forming trimers with an average diameter  $\sim 0,5 \mu\text{m}$  and a thickness 5–6 nm; each trimmer is surrounded by six others so that to form a regular hexagonal lattice [17]. The BR molecule arranged in a direction perpendicular to the plane of the cell membrane. Hydrophobic domains represent transmembrane segments and hydrophilic domains protruding from the cell membrane, connecting the individual  $\alpha$ -helical intramembraneous segments of the BR molecules.

BR acts as a light-dependent proton pump, pumping protons across the cell membrane that generates an electrochemical gradient of  $\text{H}^+$  on the surface of the cell membrane, which energy is used by the cell for the synthesis of ATP in the anaerobic photosynthetic phosphorylation. The mechanism of ATP synthesis is called “non-chlorophyll photosynthesis”, in contrast to the plant photosynthesis with the participation of chlorophyll. In this mechanism, at absorption of a light photon BR molecule became decolorized by entering into the cycle of photochemical reactions, resulting in the release of a proton to the outside of the membrane, and the absorption of proton from intracellular space. By the absorption of a light photon is occurred reversible isomerization of 13-*trans*-BR ( $\lambda_{\text{max}} = 548 \text{ nm}$ ) (the quantum yield 0,03 at +20 °C) into 13-*cis*-BR ( $\lambda_{\text{max}} = 568 \text{ nm}$ ) [18], initiating a cascade of photochemical reactions lasting from 3 ms to 1 ps with the formation of transitional intermediates J, K, L, M, N, and O, followed by separation of  $\text{H}^+$  from the retinal residue of BR and its connection from the side of cytoplasm (Fig. 6). As a result, between the internal and external surface of the membrane forms a concentration gradient of  $\text{H}^+$ , which leads that illuminated halobacteria cells begin to synthesize ATP, i.e. convert light energy into energy of chemical bonds. This process is reversible and in the dark flows in the opposite direction. In this way the BR molecule behaves as a photochromic carrier with a short relaxation



time – the transition from the excited state to the ground state. Optical characteristics of BR vary depending on the method of preparation of PM and the polymer matrix.

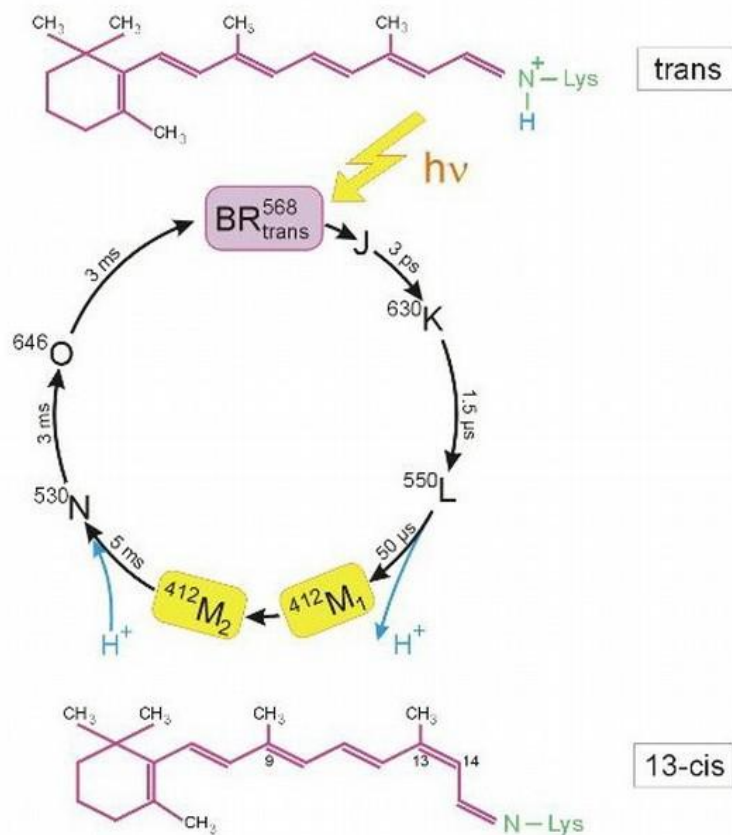


**Figure 6.** Photocycle scheme of BR (aqueous solution, pH = 7,2, t = +20 °C). Latin numbers J, K, L, M, N, O denote the spectral intermediates of BR. M<sub>1</sub> and M<sub>2</sub> represent spectral intermediants of meta- bacteriorhodopsin with the protonated and deprotonated aldimine bond. The superscripts correspond to the position of the absorption maximum of the photocycle intermediates (nm)

BR is the focus of bio- and nanotechnology because of its high sensitivity and resolution, and is used in molecular bioelectronics as natural photochromic material for light-controlled electrical regulated computer modules and optical systems [19, 20]. In addition, BR is very attractive as a model for studies related to the research of functional activity and structural properties of photo-transforming membrane proteins in the native and photo-converting membranes [21].

Nanofilms produced using the BR-containing purple membranes (PM) of halobacteria were first obtained and studied in this country in the framework of the project “Photochrome”, when it was demonstrated effectiveness and prospects for the use of BR as photochromic material for holographic recording. The main task for the manufacture of BR-containing nanofilms is the orientation of PM between the hydrophobic and hydrophilic media. Typically, to improve the characteristics of the BR-containing films use multiple layers of PM that are applied to the surface of the polymeric carrier and dried up, preserving their natural structure. The best results are achieved in the manufacture of nanofilms based on gelatin matrix [22]. This allows achieve high concentration of BR (up to 50 %) in nanofilms and avoid aggregation of membrane fragments and destruction of BR in the manufacturing process [23]. Embedded in a gelatin matrix PM fragments are durable (~10<sup>4</sup> h) and resistant to solar light, the effects of oxygen, temperatures greater than +80 °C (in water) and up to +140 °C (in air), pH = 1–12, and action of most proteases [24]. Dried PM are stacked on top of each other, focusing in the plane of the matrix, so that a layer with 1 μm thickness contains about 200 monolayers [25]. When illuminated such nanofilms exert the electric potential 100–200 mV, which coincides with the membrane potential of living cells [26]. These

factors are of great practical importance for integration of PM into polymeric nanomatrix with keeping photochemical properties.

Technology for preparation of BR consists in growing of halobacteria on liquid synthetic growth media (with 15–20 % (w/w) NaCl) with amino acids, or on natural growth media with peptons – mixtures of polypeptides and amino acids derived from the partial hydrolysis product or powdered milk, animal meat by proteolytic enzymes (pepsin, trypsin, chymotrypsin), or protein-vitamin concentrate of yeast [27]. The subsequent isolation of BR from purple membranes is carried out by a combination of physical, chemical and enzymatic methods [28]. Under optimal growing conditions (incubation period 4–5 days, temperature +35 °C, illumination with monochromatic light at  $\lambda = 560$  nm) in cells are synthesized the purple carotenoid pigment, characterized as BR by the spectral ratio of protein and chromophore fragments  $D_{280}/D_{568} = 1,5:1,0$  in the molecule.

Within the framework of the research we described an effective method for isolation of BR from PM of photo-organotrophic halobacterium *H. halobium* consisted by cellular autolysis by distilled water, processing of bacterial biomass by ultrasound at 22 KHz, llocation of PM fraction, purification of PM from low and high-molecular weight impurities, cellular RNA, carotenoids and lipids, PM solubilization in 0,5 % (w/v) solution of the ionic detergent SDS-Na to form a microemulsion with the subsequent fractionation of the protein by methanol [29]. The protein is localized in the PM; the release of low molecular weight impurities and intracellular contents is reached by osmotic shock of cells with distilled water in the cold after the removal of 4,3 M NaCl and the subsequent destruction of the cell membrane by ultrasound at 22 kHz. For the destruction of cellular RNA the cellular homogenate was treated with Rnase I. Fraction PM along with the desired protein in a complex with lipids and polysaccharides also contained impurity of related carotenoids and proteins. Therefore, it was necessary to use special methods of fractionation of the protein without damaging its native structure and dissociation.

BR being a transmembrane protein intricately penetrates bilipid layer in form of seven  $\alpha$ -helices; the use of ammonium sulfate and other conventional agents to salting out did not give a positive result for isolation of the protein. The resolving was in the translation of the protein to a soluble form by the colloidal dissolution (solubilization) in an ionic detergent. Using as the ionic detergent SDS-Na was dictated by the need of solubilization of the protein in a native, biologically active form in complex with 13-*trans*-retinal, because BR solubilized in 0,5 % (v/v) SDS-Na retains a native  $\alpha$ -helical configuration [30]. Therefore, there is no need the use organic solvents as acetone, methanol and chloroform for purification of lipids and protein, and precipitation and delipidization are combined in a single step, which significantly simplifies the further fractionation. A significant advantage of this method is that the isolated protein in complex with lipids and detergent molecules was distributed in the supernatant, and other high molecular weight impurities – in unreacted precipitate, easily separated by centrifugation. Fractionation of solubilized in 0,5 % (w/v) SDS-Na protein and its subsequent isolation in crystalline form was achieved at 0 °C in three steps precipitating procedure with methanol, reducing the concentration of detergent from 0,5; 0,25 and 0,1 % (w/v) respectively. The final stage of BR purification involved the separation of the protein from low-molecular-weight impurities by gel-permeation chromatography on dextran Sephadex G-200 Column balanced with 0,09 M Tris-HCl buffer ( $pH = 8,35$ ) with 0,1 % (w/v) SDS-Na and 2,5 mM EDTA (output of the protein 8–10 mg).

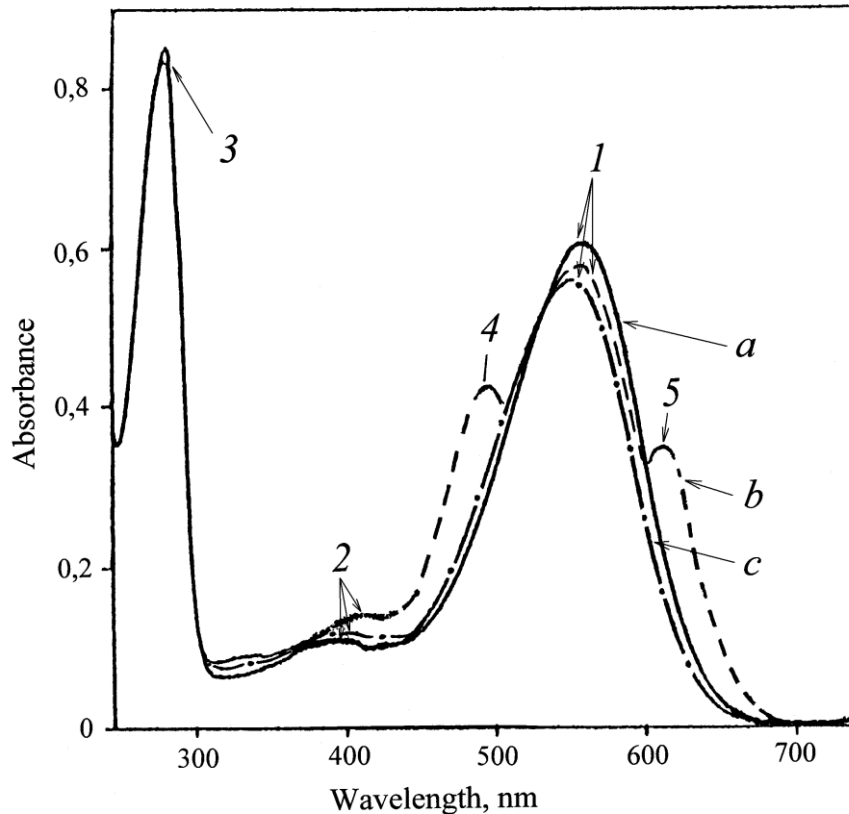


Figure 7. The absorption spectra of the PM (50% (v/v) ethanol) at various stages of processing: (a) – natural BR; (b) – PM after intermediate treatment; (c) – PM purified from carotenoids. The bandwidth (1) is the spectral form of BR<sup>568</sup>, (2) – impurity of spectral form of *meta*-bacteriorhodopsin (M<sup>412</sup>), (3) – the total absorption bandwidth of aromatic amino acids, (4) and (5) – extraneous carotenoids. As a control used the native BR

Absorption spectra of PM purified from carotenoids (4) and (5) (chromatographic purity 80–85 %) are shown in Figure 7 at various processing stages (b) and (c) relative to the native BR (a). Formation of retinal-protein complex in the BR molecule leads to a bathochromic shift in the absorption spectrum of PM (Fig. 8c) – the main bandwidth (1) with the absorption maximum at  $\lambda = 568$  nm caused by the light isomerization of the chromophore by the C13=C14 bond is determined by the presence of 13-*trans*-retinal residue in BR<sup>568</sup>; additional low-intensity bandwidth (2) at  $\lambda = 412$  nm characterizes a minor impurity of a spectral form of *meta*-bacteriorhodopsin (M<sup>412</sup>) (formed in the light) with deprotonated aldimine bond between 13-*trans*-retinal residue and protein; the total bandwidth (3) with  $\lambda = 280$  nm is determined by the absorption of aromatic amino acids in the polypeptide chain of the protein (for native BR  $D_{280}/D_{568} = 1,5 : 1,0$ ).

The final stage of BR purification involved the separation of the protein from low-molecular-weight impurities by gel-permeation chromatography (GPC). For this purpose the fractions containing BR were passed twice through a chromatography column with dextran Sephadex G-200 balanced with 0,09 M Tris-buffer (pH = 8,35) containing 0,1% (w/v) SDS-Na and 2,5 mM EDTA. Elution was carried out at  $20 \pm 25$  °C with 1 mM Tris-HCl buffer (pH = 7,6) at 10 ml/cm<sup>2</sup>·h. The data on purification of BR of phospholipids and carotenoids are shown in Table 1. 84% of phospholipids was removed by five washes (65, 70 and 76% was removed by 1st, 2nd and 3rd wash respectively). The total endogenous phospholipid removal on the BR peak was 92% relative to the native PM.

Table 1: Summary results for the isolation and purification of BR by various methods

| Sample                           | PM content,<br>mol PM/mol BR | Phospholipid and<br>carotenoid<br>removal, % | BR yield*, % |
|----------------------------------|------------------------------|--|--------------|
| PM fraction                      | 20,5                         | –  | –            |
| PM washed with EtOH              |                              |  |              |
| 1 wash                           | 16,9                         | 65   | 93           |
| 2 wash                           | 15,1                         | 70   | 90           |
| 3 wash                           | 14,5                         | 76   | 88           |
| 4 wash                           | 13,6                         | 81   | 84           |
| 5 wash                           | 13,2                         | 84   | 80           |
| BR crystallised from<br>MeOH     | 12,9                         | 86   | 75           |
| BR from GPC on<br>Sephadex G-200 | 10,2                         | 92   | 86           |

\* Notes: Percentage yield is indicated in mass.% relative to BR solubilized in 0,5% SDS-Na before concentration.

The method for protein fractionation made it possible to obtain 8–10 mg of BR from 1 g of bacterial biomass. The homogeneity of BR was confirmed by electrophoresis in 12,5% (w/v) PAAG with 0,1% (w/v) SDS-Na and the regeneration of apomembranes with 13-*trans*-retinal.

### **Iodopsin**

Iodopsin is a violet, light-sensitive pigment of the retinal cone cells, responsible for the light and color vision in mammals, the close analogue of rhodopsin. This pigment consists of a protein named photopsin linked with the chromophore, a retinal residue. According to the three-component theory of vision, it is believed that there has to be three types of this pigment and accordingly – three types of cones that are sensitive to blue, green and red light correspondingly. Evidently, there should be three types of cones – S, M, L types, each of which contains only their photosensitive pigment, corresponding to a specific opsin.

It is now established that this group of pigments comprises the isomorphic pigments, slightly different in composition and absorption spectra. Various opsins are different by amino acids in the molecule, and absorb light at several different wavelengths as do retinal-related molecules.

Iodopsin consists of three pigments – hlorolab, eritrolab and tsianolab. With the densitometry method W. Rushton studied the coefficient of light absorption in the photo layers of the retina with different wavelengths [31]. The hlorolab pigment absorbs the light rays corresponding to yellow-green (450–630 nm absorption band), the eritrolab – yellow and red ( $\lambda = 500-700$  nm), and the third predicted pigment tsianolab – blue-green ( $\lambda = 500-700$  nm) parts of the visible spectrum [32]. However, other different types of cones containing the only one pigment have not still yet been found.

The applying of intensive adapting yellow, purple and blue background, allowed get three different threshold curves in absorption spectra of iodopsin [33]. Making a correction for light absorption by the front media of the eye (lens and macular pigment yellow), G. Wald indicates as the maximums of the three pigments the peaks corresponding to the wavelengths:  $\lambda = 430, 540$  and 575 nm, which correspond to the photoreceptors cones of the retina that produce basic bio-signals – S, M, L (Table 2).

Table 2: The maximums of tsianolab, hlorolab and eritrolab pigments in absorption spectra and the sensitivity range [33]

| Type of cones/photopigment (opsin) | Designation | Sensitivity range | Maximum sensitivity |
|------------------------------------|-------------|-------------------|---------------------|
| S-cones/tsianolab (OPN1SW)         | $\beta$     | 400–500 nm        | 420–440 nm          |
| M-cones/hlorolab (OPN1MW)          | $\gamma$    | 450–630 nm        | 534–545 nm          |
| L-cones/eritrolab (OPN1LW)         | $\rho$      | 500–700 nm        | 564–580 nm          |

It should be noted, however, that this interpretation does not fit correctly into the very basis of three-component hypothesis of color, as eritrolab and hlorolab have a sensitivity to the entire visible spectrum, and according to the three-component hypothesis they should be the narrow channeled, and their spectra sensitivity must comply strictly to the certain regions of the spectrum. In addition their maximums do not correspond to red and green colors (as postulated by the three-component hypothesis); their actual spectral maxima correspond to eritrolab – yellow-red (orange) and hlorolab – yellow-green region of the spectrum.

**The basic principles of the mechanism of color vision**

It is established that the retina has three types of cone cells – S, M and L cells, having a different sensitivity to different parts of the visible range of the spectrum (Fig. 8). The cone cells of S type have a spectral range from  $\lambda = 400$  nm to  $\lambda = 500$  nm with a maximum peak at  $\lambda = 420$ –440 nm, the cone cells of M type – from  $\lambda = 450$  nm to  $\lambda = 630$  nm with a maximum peak at  $\lambda = 534$ –555 nm, while the cone cells of L type – from  $\lambda = 500$  nm to  $\lambda = 700$  nm with a maximum peak at  $\lambda = 564$ –580 nm. As the curves of the sensitivity of the cone cells overlap, it is impossible for the monochromatic light to stimulate only one type of cone cells. The other types of cone cells react though to a lesser degree. The set of all possible values of the color combinations causing a visual reaction determines the human color space. The human brain generally can discern approximately 10 million of different colors.

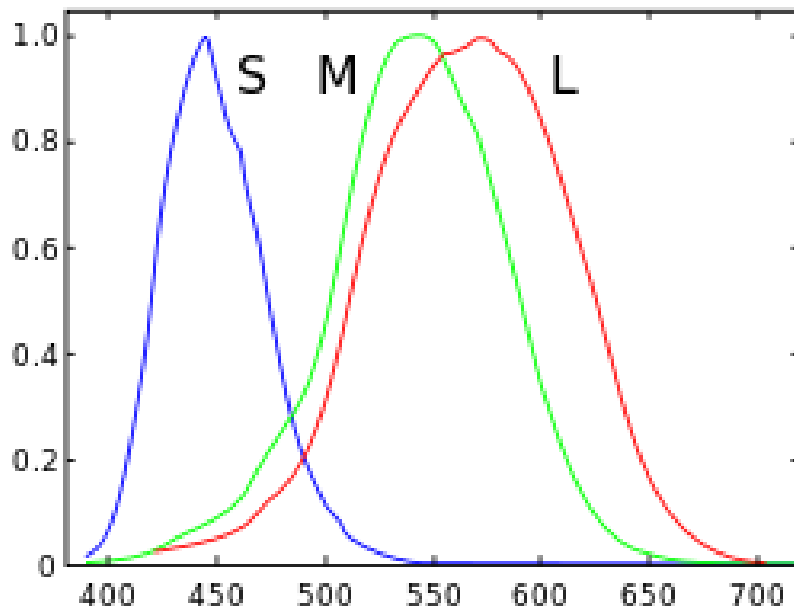


Figure 8. The spectra of blue, green, and red rays in S, M and L points on the graphs of electromagnetic waves, which cones emit as the brightest ray signals rays of these points, from all the beams of monochromatic waves of substantive focused points with lengths in nm.

The electromagnetic wave spectrum stimulates the different types of cone cells from the three types S, L and M to a different degree. Thus, the red light stimulates the L cone cells more than the

M cone cells. On the contrary, the blue light stimulates the S cone cells in the strongest way. The yellow-green light provides a strong stimulation to the L and M cone cells, and a weaker stimulation to the S cone cells. The brain then combines the information from all types of cone cells for different wavelengths and analyzes them as different colours.

### ***The additive mixing of colors***

The analysis of the activity of the three types of cones – S, L and M in the perception of different colors also shows how the brain “deciphers” the different colors. The foundation of this colour analysis, shown in Figure 10, was made by M. Marinov and I. Ignatov in 2008. The maximum of the spectral sensitivity of the visual analyzer corresponds to the light green colour corresponds to 560 nm in spectra (Fig. 9). However, it is not clear whether the green colour perceived by brain is a combined mixing effect of the yellow and blue colors, or whether it corresponds to a wavelength of the green color from the visible spectrum. The human brain can register the colors, i.e. the green colour as a spectrometer, with certain lengths of the electromagnetic waves. It can also register the green colour as a mixture of yellow and blue. However, the full perception of colours by the visual analyzer cannot be defined by a spectrometer.

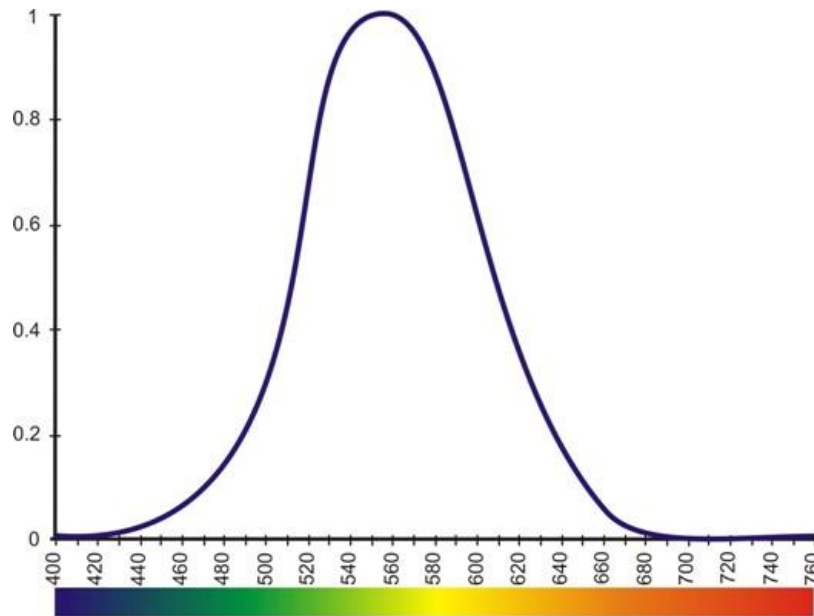


*Figure 9.* The maximum of the spectral sensitivity of the visual analyzer on the graphs of the electromagnetic waves (M. Marinov and I. Ignatov, 2008)



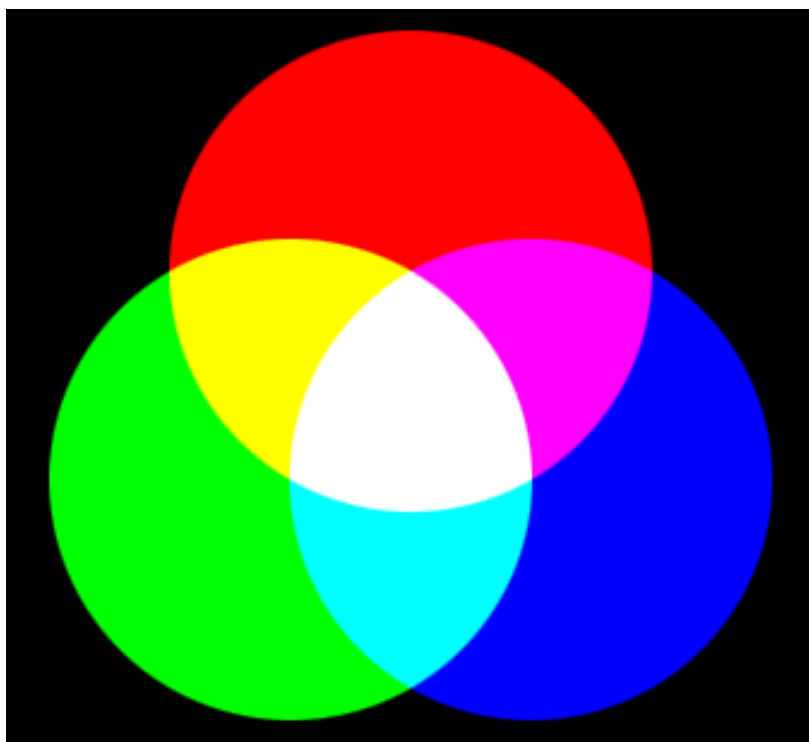


Figure 10. Additive physical mixing of different colours by the visual analyzer (M. Marinov and I. Ignatov, 2008)

As an example via the mixing of electromagnetic waves that correspond to green and red colour, the medium yellow colour is obtained. In the mixing process of green and red, no medium colour is obtained; the brain therefore perceives it as the yellow colour [34]. When there is an emission of electromagnetic waves that correspond to green and red colour, the brain adopts an “average decision” – the yellow colour (Fig. 10). Analogously, for the yellow and blue colour, the brain adopts an “average decision” – the green colour. This means that a spectral mixing of colours is observed between the blue-yellow and green-red pairs [35]. In its turn, green and blue colours are perceived as the cyan colour. The vision sensitivity furthermore is at its lowest for the violet, blue and red color. The mixing of electromagnetic waves that correspond to the blue and red colour is perceived as the violet colour. In the mixing of electromagnetic waves that correspond to more colors, the brain does not perceive them as separate or average, but as a white colour. Thus, the spectral notion of colour is not determined solely by the wavelength. The analysis is being performed by brain, and the notion of colour is at its essence a product of our consciousness.

### Conclusions

The mechanism of color perception by the visual analyzer has been studied using a photoreceptive chromo-protein rhodopsin as a basic model. A further research into the function of rhodopsin and other retina affiliated chromo-proteins as iodopsin will allow investigate in detail the mechanism of visual perception of light for better treatment of functional eye diseases in ophthalmology. It should be noted that rhodopsin up till now remains to be the most studied model chromoprotein of all GPCR-receptor family. This allowed us to us to carry out the comparative analysis and better analyze the functional properties of another analogous trans-membrane bacterial chromoprotein – bacteriorhodopsin isolated from purple membranes of halobacterium *H. Halobium ET 1001* in semi-preparative quantities, and study its structural-functional parameters and applications in bio-nanotechnologies.

### Acknowledgements

The authors wish to thank Parashkeva Tzaneva (Bulgarian Academy of Science) for her cooperation in the research. Also authors would like to commemorate the memory of Prof. Marin Marinov (1928–2009) – the initiator of the research of color vision in Bulgaria.

**References:**

1. Neugebauer D.Ch. Recrystallization of the purple membrane *in vivo* and *in vitro* / D.Ch. Neugebauer, H.P. Zingsheim, D. Oesterhelt // Journal Molecular Biology. 1978. Vol. 123. P. 247–257.
2. Rudiger M. Reconstitution of bacteriorhodopsin from the apoprotein and retinal studied by Fourier-transformed infrared spectroscopy / M. Rudiger, J. Tittor, K. Gerwert, D. Oesterhelt // Biochemistry. 1997. Vol. 36. P. 4867–4874.
3. Hubel D. Eye, Brain and Vision. Scientific American Library Series (Book 22), 2nd edition, New York: W.H. Freeman Publ., 1995. 256 p.
4. Hogan M.J. Histology of the Human Eye / M.J. Hogan, J.A. Alvarado, J.E. Weddell. Philadelphia: WB Saunders Co., 1970. 115 p.
5. Nathans J. Molecular genetics of human color vision: the genes encoding blue, green, and red pigments / J. Nathans, D. Thomas, D.S. Hogness // Science. 1986. Vol. 232, № 47. P. 193–202.
6. Liang Y. Rhodopsin signaling and organization in heterozygote rhodopsin knockout mice / Y. Liang, D. Fotiadis, T. Maeda // J. Biol. Chem. 2004. Vol. 279. P. 48189–48196.
7. Palczewski K., Kumasaka T., Hori T. Crystal structure of rhodopsin: a G-protein-coupled receptor // Science. 2000. Vol. 289. P. 739–745.
8. Henderson R. Model for the structure of bacteriorhodopsin based on high-resolution electron cryo-microscopy / K. Palczewski, T. Kumasaka, T. Hori // J. Mol. Biol. 1990. Vol. 213, № 4. P. 899–929.
9. Palczewski K. G-protein-coupled receptor rhodopsin / K. Palczewski // Annu. Rev. Biochem. 2006. Vol. 75. P. 743–767.
10. Ovchinnikov Yu.A. Visual rhodopsin: Whole amino acid sequence and topology in membrane / Yu.A. Ovchinnikov, N.G. Abdulaev, M.Yu. Feigina, I.D. Artamonov, A.S. Bogachuk // Bioorganic. Chemistry. 1983. № 10. P. 1331–1340.
11. Hargrave P.A. The structure of bovine rhodopsin / P.A. Hargrave, J.H. McDowell, D.R. Curtis // Biophys. Struct. Mech. 1983. Vol. 9. P. 235–244.
12. Schertler G.F. Projection structure of frog rhodopsin in two crystal forms / G.F. Schertler, P.A. Hargrave // Proc. Natl. Acad. Sci. U.S.A. 1995. Vol. 92. P. 11578–11582.
13. Lipkin V.M. Visual system. mechanisms of transmission and amplification of the visual signal in eye retina / V.M. Lipkin // Soros Educational Journal. 2001. Vol. 7, № 9. P. 2–8 [in Russian].
14. Oesterhelt D. Rhodopsin - like protein from the purple membrane of *Halobacterium halobium* / D. Oesterhelt, W. Stoeckenius // Nature. 1971. Vol. 233, № 89. P. 149–160.
15. Lanyi J.K. X-ray diffraction of bacteriorhodopsin photocycle intermediates / J.K. Lanyi // Molecular Membrane Biology. 2004. Vol. 21, № 3. P. 143–150.
16. Jap B.K. Peptide-chain secondary structure of bacteriorhodopsin / B.K. Jap, M.F. Maestre, S.B. Hayward, R.M. Glaeser // Biophys J. 1983. Vol. 43, № 1. P. 81–89.
17. Nonella M. Structure of Bacteriorhodopsin and in situ isomerization of retinal: A molecular dynamics study / M. Nonella, A. Windemuth, K. Schulten // Journal Photochem. Photobiol. 1991. Vol. 54, № 6. P. 937–948.
18. Zimanyi L. Pathway of proton uptake in the bacteriorhodopsin photocycle / L. Zimanyi, Y. Cao, R. Needleman, M. Ottolenghi, J.K. Lanyi // Biochemistry. 1993. Vol. 32. P. 7669–7678.
19. Vought B.W. Molecular electronics and hybrid computers / B.W. Vought, R.R. Birge R.R. (Eds.) in: Wiley Encyclopedia of Electrical and Electronics Engineering. NY: Wiley-Interscience, 1999. 490 p.
20. Hampp N. Bacteriorhodopsin and its potential in technical applications / N. Hampp, D. Oesterhelt. in: Nanobiotechnology / Ch. Niemeyer, C. Mirkin (eds.). Weinheim: Wiley-VCH-Verlag, 2004. 167 p.
21. Wang W.W. Bioelectronic imaging array based on bacteriorhodopsin film / W.W. Wang, G.K. Knopf, A.S. Bassi // IEEE Transactions on Nanobioscience. 2008. Vol. 7, № 4. P. 249–256.
22. Shuguang W.U. Bacteriorhodopsin encapsulated in transparent sol-gel glass: a new biomaterial / W.U. Shuguang, L.M. Ellerby, J.S. Cohan // Chem. Mater. 1993. Vol. 5. P. 115–120.
23. Weetall H. Retention of bacteriorhodopsin activity in dried sol-gel glass / H. Weetall // Biosensors & Bioelectronics. 1996. Vol. 11. P. 325–333.

24. Downie J. Long holographic lifetimes in bacteriorhodopsin films / J. Downie, D.A. Timucin, D.T. Smithy, M. Crew // Optics Letters. 1998. V. 23, № 9. P. 730–732.
25. Korposh S.O. Films based on bacteriorhodopsin in sol-gel matrices / S.O. Korposh, M.Y. Sichka, I.I. Trikur // Proc. of SPIE. 2005. Vol. 5956. Paper Number 595616. P. 312–320.
26. Seitz A. Kinetic optimization of bacteriorhodopsin films for holographic interferometry / A. Seitz, N. Hampp // J. Phys. Chem. B. 2000. Vol. 104, № 30. P. 7183–7192.
27. Mosin O.V. The inclusion of deuterated aromatic amino acids in the molecule of bacteriorhodopsin *Halobacterium halobium* / O.V. Mosin, D.A. Skladnev, V.I. Shvets // Applied Biochemistry and Microbiology. 1999. Vol. 35, № 1. P. 34–42.
28. Mosin O.V. Biosynthesis of transmembrane photo transforming protein bacteriorhodopsin labeled with deuterium on residues of aromatic acids [2,3,4,5,6-<sup>2</sup>H<sub>5</sub>]Phe, [3,5-<sup>2</sup>H<sub>2</sub>]Tyr and [2,4,5,6,7-<sup>2</sup>H<sub>5</sub>] / O.V. Mosin, V.I. Shvez, D.A. Skladnev, I. Ignatov // Nauchnoe priborostroenie. 2013. Vol. 23, № 2. P. 14–26 [in Russian].
29. Mosin O.V. The photo-transforming photochrome protein bacteriorhodopsin derived from photoorganoheterotrophic halobacterium *Halobacterium halobium* / O.V. Mosin, I. Ignatov // Nanoengineering. 2013. Vol. 1. P. 14–21 [in Russian].
30. Mosin O.V. The natural photo-transforming photochrome transmembrane protein nanomaterial bacteriorhodopsin from purple membranes of halobacterium *Halobacterium halobium* / O.V. Mosin, I. Ignatov // Journal of Nano and Microsystem Technique. 2013. Vol. 7. P. 47–54 [in Russian].
31. Rushton W.A.H. In: Visual problems of colour / N.P.L. Sump. (Ed.) London: Her Majesty's Stationary Office, 1958. Vol. 1. P. 71–101.
32. Wyszecki G. Color Science: Concepts and Methods, Quantitative Data and Formulae (2nd ed.) / G. Wyszecki G., W.S. Stiles. New York: Wiley–IS&T Series in Pure and Applied Optics, 1982. 935 p.
33. Wald G. The receptors of human color vision // Science. 1964. Vol. 145 (3636). P. 1007–116.
34. Ignatov I. Process of perception of light and evolution of sight at the higher animals and humans / I. Ignatov, O.V. Mosin // Naukovedenie. 2013. № 3. P. 1–19 [in Russian], [Online] Available: URL: <http://naukovedenie.ru/PDF/98tvn313.pdf> (May-June 2013).
35. Ignatov I. Color Kirlian spectral analysis. Color observation with visual analyzer / I. Ignatov, M. Marinov // Euromedica, 2008. 32 p.